17th World Conference on Earthquake Engineering, 17WCEE
Sendai, Japan - September 13th to 18th 2020

CHARACTERIZATION AND NUMERICAL ASSESSMENT OF LEAD EXTRUSION DAMPER WITH ADAPTIVE BEHAVIOR

E. Bruschi(1), F. Macobatti(2), C. Pettorruso(3), V. Quaglini(4)

(1) *PhD Student, Politecnico di Milano, Department of Architecture, Built Environment and Construction Engineering, eleonora.bruschi@polimi.it*
(2) *Research Fellow, Politecnico di Milano, Department of Architecture, Built Environment and Construction Engineering, fabio.macobatti@polimi.it*
(3) *PhD Student, Politecnico di Milano, Department of Architecture, Built Environment and Construction Engineering, carlo.pettorruso@polimi.it*
(4) *Associate Professor, Politecnico di Milano, Department of Architecture, Built Environment and Construction Engineering, virginio.quaglini@polimi.it*

Abstract

Supplemental energy dissipation or damping systems are worldwide employed both in new and retrofit constructions in order to prevent structural damage, increase life-safety and achieve a desired level of performance A large number of devices have been developed in the past years, characterized by either hysteretic or viscous behavior. Despite substantial differences exist, all these devices are used with the philosophy of limiting or eliminating damage to the structural frame by dissipating much of the energy imparted by ground motion in elements not forming part of the gravity framing system.

In this study a Lead Extrusion Damper (LED) has been experimentally and numerically investigated in the study. The device provides a resistive force by plastically extruding lead through an orifice created by an annular restriction between a tube and a bulged shaft.

Cyclic tests according to EN 15129 were performed to obtain the basic characteristics of the LED for different displacement amplitudes. The damper exhibits a consistent rigid-plastic behavior without significant strength degradation; the shape of the hysteresis loops is essentially rectangular, resulting in an equivalent damping ratio of 0.55. The tested specimen was able to sustain multiple sequences of motion at the basic design earthquake displacement, demonstrating its ability to provide maintenance-free operation even in presence of repeated ground shakes.

A 3D finite element model of the LED was formulated and used in a parametric study to investigate the distinct effects of the shaft diameter and the bulge diameter on the strength of the device. It is shown that the main parameter governing the response of the LED is s the annular area of the bulge that represents the projected face area of the bulge over which direct stress is applied to the shaft The results of the parametric study can be used to draw design charts to assist the manufacturers for the preliminary design of the system.

Eventually, a novel Adaptive Lead Extrusion Damper (ALED) was assessed in preliminary tests. The ALED provides a “two-steps” rigid-plastic loop, with a substantial increase in the resisting force when a certain displacement is exceeded. Thereby the ALED could be used in structures to effectively modify their response depending on the magnitude of the ground motion.

Keywords: Lead Extrusion Damper, rigid-plastic hysteretic loop, adaptive response, experiments, time history analyses

1. Introduction

The concept of using supplemental systems to increase the damping in a structure was suggested in the late '60s of the twentieth century [1-3]. Its philosophy consists in eliminating or limiting damage to the structure by concentrating the dissipation of much of the seismic energy in elements out of the gravity framing system. Nowadays supplemental energy dissipation or damping systems are worldwide employed both in new and retrofitted constructions in order to prevent structural damage, increase life-safety and achieve a desired level of performance.

Current energy dissipation devices can be classified in two main categories [4]. The first one includes the so-called fluid viscous dampers, where the dissipation is achieved through the lamination of a viscous fluid forced by a piston to pass through an orificing or valving system. The behavior of these devices strictly depends on the fluid velocity. Viscous fluid dampers are very versatile and can be designed to allow unconstrained slow motions (like e.g. thermal motions) as well as provide controlled damping of a structure to protect from wind load or earthquakes. The second category is represented by hysteretic dampers, which are further classified in hysteretic steel dampers, friction dampers and metal extrusion dampers, depending on the mechanism actually used to dissipate the seismic energy. Most of the dampers used in residential, school and industrial buildings belong to the hysteretic damper's category, whose constitutive law is strictly dependent on the accommodated displacement. The theoretical force – displacement curves of hysteretic dampers are shown in Fig. 1, where N_D is the axial force and Δ_D is the axial displacement of the damper, and N_y is the yield strength of the device; the area included in the curves corresponds to the energy dissipated by the device during a cycle.

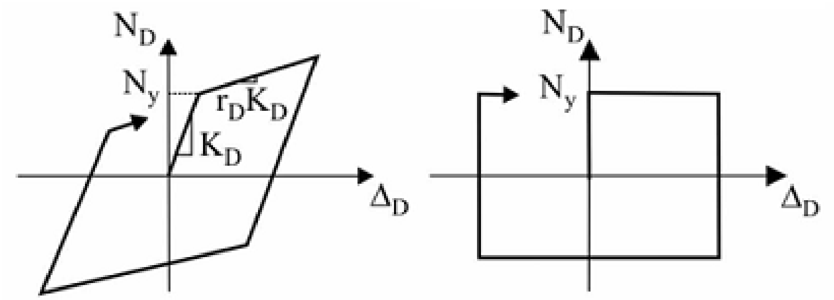

Fig. 1 – Theoretical hysteresis loops of hysteretic dampers: left, steel dampers; right, friction dampers and extrusion dampers

Supplemental energy dissipation is typically implemented by providing the structure with dissipative bracing systems, made of steel braces equipped with dissipation devices. This approach is aimed at achieving two effects, namely increase the structural stiffness, with consequent reduction of displacements, and dissipate much of the seismic energy, leading to a reduction of the accelerations.

However, though in principle dissipative braces represent a viable solution to protect any kind of building, this approach is affected from some drawbacks such as increased internal forces in beams and columns, modification of the building layout, and in case of retrofit, the need of a significant amount of construction work, resulting in heavy disturbance to the occupants. Supplemental energy dissipation is indeed mainly used for new constructions, where the provision of the dissipative braces can be planned since the beginning, rather than for retrofit, because of architectural issues posed by the braces, like interference with the design of the façade and position of the openings. A further issue concerns the fact that the energy dissipation mechanism is engaged when the earthquake-induced dynamic force in the system exceeds the yield force N_y (Fig. 1), associated to e.g., yielding of a steel core or static friction between sliding surfaces; indeed, in case of small or moderate earthquakes the damper may be not engaged, failing to protect the structural frame. On the contrary, after their engagement during a strong seismic event, hysteretic devices usually require to be restated or replaced, with a consequent economic burden but also with an impact on the safety of the structure, which is left exposed to aftershocks.

In conclusion, current hysteretic dampers seem not capable to fully match the requirements of a resilient community. An optimal earthquake-resistant system should incorporate the constitutive behavior of existing devices in a more compact and architecturally less invasive design; they also should not require maintenance after a major earthquake, in order to guarantee a high safety level and maintain an economical appeal, especially for the retrofitting of conventional buildings, such as residential, school and industrial buildings.

A hysteretic dissipation system that deserves a deeper analysis is the Lead Extrusion Device, or LED [5]. In this device the dissipation of seismic energy is achieved by forcing the plastic extrusion of lead through an orifice created by an annular restriction within a tube (Fig. 2). Lead Extrusion Dampers have been reported to present an essentially rectangular hysteretic curve, which maximizes the amount of energy dissipation for a given applied force and displacement [5-11]. Moreover, LEDs feature other desirable characteristics, such as a stable and repeatable behavior, an insignificant sensitivity to aging and environment, compact dimensions, and low cost.

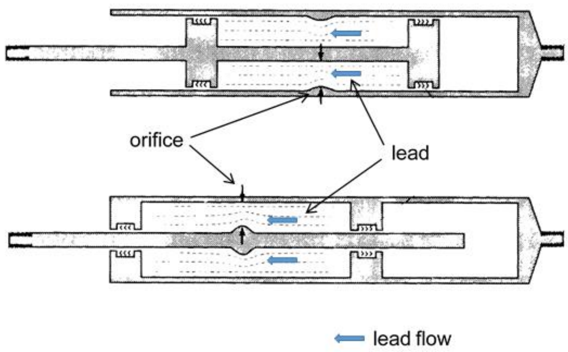

(a)

(b)

Fig. 2 – Longitudinal sections of two versions of the LED: (a) constricted tube type; (b) bulged shaft type. Adapted from [12]

This paper presents an experimental and numerical investigation of the LED. First, a prototype of LED is manufactured and tested in order to verify its compliance to the provisions of the European standard EN 15129 [13] for Displacement Dependent Devices, and additional tests are performed in order to check the ability of the system to resist multiple sequences of shaking without deterioration of its mechanical characteristics. A 3D model of the LED is then formulated in a finite element code and used in a parametric analysis to establish simple design rules. Eventually, preliminary tests on a novel version of LED with adaptive behavior are presented and commented.

2. Lead extrusion dampers

LEDs were first introduced as a passive energy dissipation device in the mid '70s in New Zealand [6, 14, 15]. The basic principle of the device is illustrated in Fig. 2. The lead is confined into a tube where an orifice is created by an annular restriction, which can be achieved either through a constriction of the tube (Fig. 2a), or a bulged shaft (Fig. 2b). As the shaft is forced through the tube, the lead is forced to flow through the annular restriction. This plastic flow adsorbs a large amount of energy, due to the shearing and deformation of the material [16], providing high resistive forces. A part of the energy required to produce the plastic deformation of lead is immediately dissipated as heat, while some of the energy is stored in the deformed lead and it drives three interrelated processes which are called recovery, recrystallization and grain growth, which tend to restore the lead to its original condition [17, 18].

The amount of energy that can be dissipated by the LED is limited by two major factors. First, the yield force of the device is restricted by the load capacity of the shaft, which is in turn defined by practical limits on shaft diameter and manufacturing and cost limitations on shaft material. Second, the heat produced by the damper on repeated cycles softens the lead and reduces the yield resistance and the bulk compressibility of the material. Both factors can be reasonably managed by design [6]. Another practical issue with LED has been reported to be the formation of voids within the working material during extrusion. The void formation can be ascribed to casting porosity, compression of the lead, and expansion of the confining tube wall. Hence, as the shaft moves, the material is compressed into a smaller volume, leaving a trailing void. As the bulge passes through this void at motion reversals on subsequent cycles, the damper experiences less resistance and dissipates less energy.

3. Experimental investigation

3.1 LED prototype

A bulged-shaft type LED design is adopted in this study (Fig. 3). The LED comprises four main components, namely the bulged shaft, the tube, the threaded cap and the lead, which is used to fill the void between the tube and the shaft. Tube, shaft and cap are made of structural steel. In accordance to previous studies [9, 10], the diameters of the shaft and the bulge are set to 32 mm and 42 mm, respectively, and the inner diameter of the tube is 60 mm, resulting in a clearance between the bulge and the tube of 9 mm. The design displacement of the prototype is 20 mm in either direction. A bushing is provided in the cap to prevent leakage of lead around the shaft. To reduce casting porosity and minimize void formation, the lead is prestressed during the assembly of the device by tightening the cap with a controlled torque.

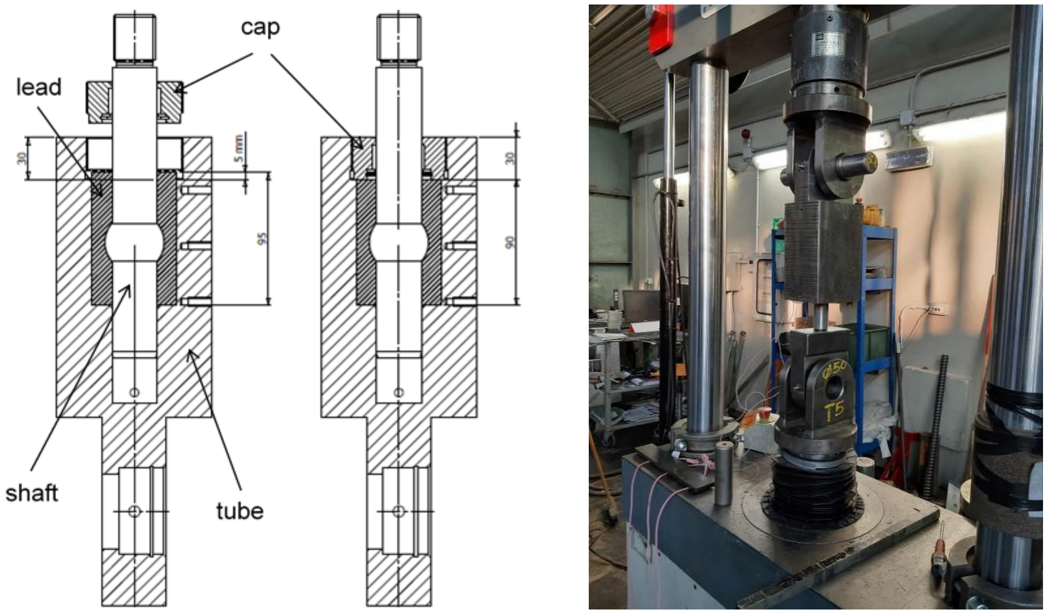

(a) (b)

Fig. 3 – (a) Assembly of the bulged-shaft LED; (b) specimen on the testing machine

3.2 Experimental protocol

The LED was tested at the Materials Testing Laboratory of Politecnico di Milano, using a 500 kN servohydraulic testing machine. Three thermocouples were inserted in as many blind holes drilled in the tube wall to monitor the temperature rise during sustained cycling.

The specimen was subjected to the testing protocol established in the European standard on antiseismic devices [13] for Displacement Dependent Devices. The hysteretic force-displacement response was evaluated by imposing cycles of increasing amplitude at 25%, 50% and 100 % of the design displacement. Five cycles for each intermediate amplitude and ten cycles for the maximum amplitude were applied. The loading frequency was 0.5 Hz. Then, a ramp test to the design displacement multiplied by an amplification factor $\gamma_b = 1.1$ and by a reliability factor $\gamma_x = 1.2$ was performed at a velocity of 0.1 mm/s, to assess the failure condition under static condition. Eventually, though not required by the standard, a second series of 10 consecutive cycles at the maximum displacement was performed after the ramp test to evaluate the ability of the device to survive multiple loading sequences.

3.3 Results

The specimen exhibits almost optimal rectangular hysteresis loops, with only small "cut-outs" from the corners due to the effects of the trailing void (Fig. 4a). Indeed, after the cut-out, the peak force stabilizes at an essentially steady level, thus maximizing the amount of energy dissipation. From the shape of the hysteresis loop the length of the trailing void created behind the bulge is estimated to be approximately 7 mm over a total stroke of 40 mm. The yield strength N_y tends to decrease as the number of cycles increases due to heating of lead (Fig 4b); the maximum force passes from 205 kN at the first cycle to 170 kN at the tenth cycle when the device works in extension ($N_y > 0$), and from 243 kN to 193 kN when the device works in compression ($N_y < 0$). The observed asymmetric behavior is ascribed to the compliance of the threaded cap, that creates an extra volume that lead can fill rather than flow through the annular orifice around the bulge.

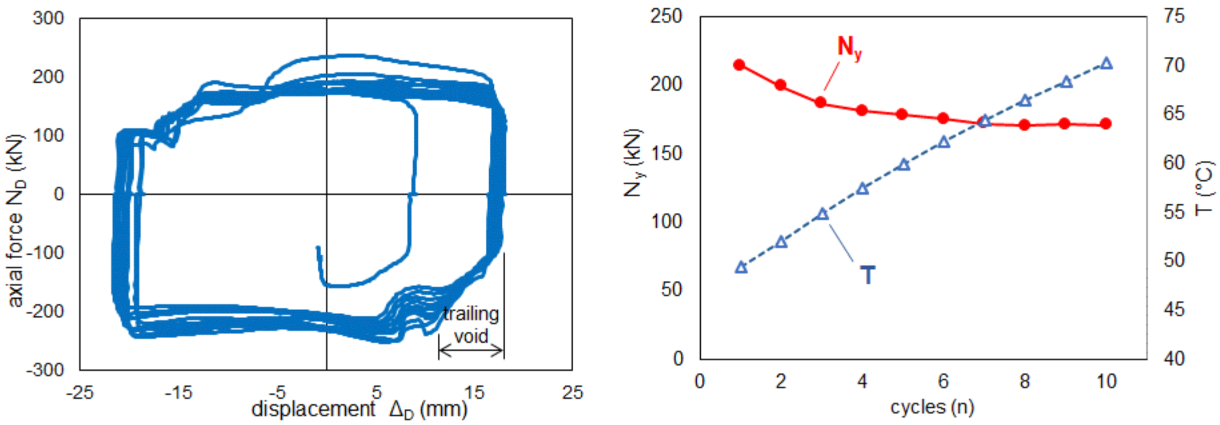

(a) (b)

Fig. 5 – (a) Hysteresis loops of the LED specimen tested to 100% of design displacement; (b) progress of (average) yield force and temperature within the tube wall vs. number of cycle

Two quantities are calculated at each cycle and used to characterize the response of the LED, namely the effective stiffness and the equivalent damping ratio

$$K_{eff} = \frac{N_y}{\Delta_m} \qquad \xi_{eff} = \frac{2}{\pi} \cdot \frac{A_{cycle}}{4K_{eff} \cdot \Delta_m} \tag{1}$$

where N_y is the yield force (determined as the average between the absolute values measured on the positive and the negative branches of the loop), Δ_m is the maximum displacement of the cycle, and A_{cycle} is the area of the histeresis loop, i.e. the amount of energy dissipated on a cycle.

As shown in Fig. 5, when the first cycle is disregarded, both quantities remain essentially constant during the sequence of cycles, hence satisfying the stability requirement provided in the standard [13]. The average value of ξ_{eff} on the 10 cycles performed to the design displacement is 0.55, i.e. 86% of the theoretical value provided by a rectangular loop, confirming the good dissipating capacity of the LED. The parameters evaluated on two sequences of 10 cycles each at the design displacement overlap: after cooling down to ambient temperature lead recristallizes and recovers its original properties, thereby providing a reliable and consistent response even in case of multiple loading sequences. Eventually, in the ramp test (data not shown) the specimen was able to accomodate the amplified design displacement by providing a consistent response up to 24.6 mm.

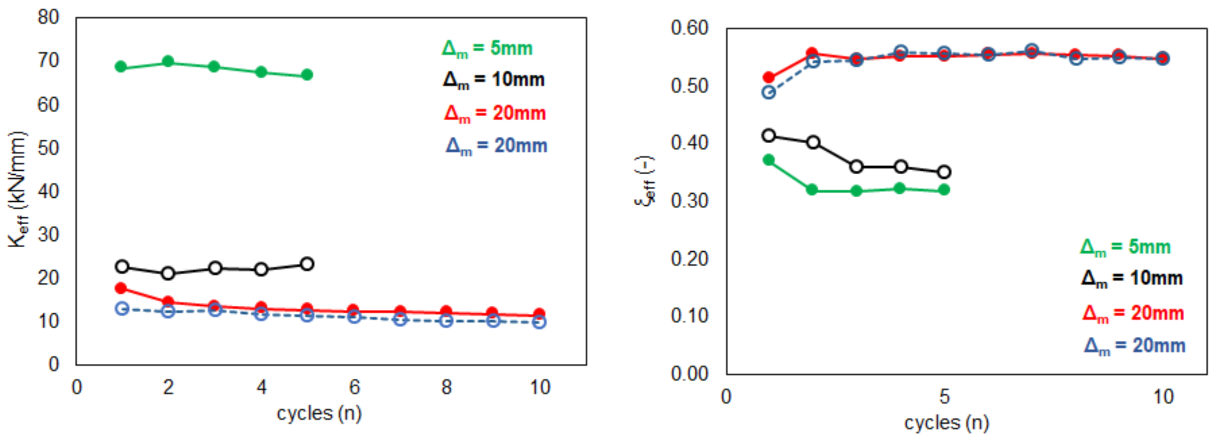

(a) (b)

Fig. 5 – Evaluation of effective stiffness and equivalent damping ratio at different displacement amplitudes

4. Numerical analyses

4.1 Numerical model

A 3D finite element model of the LED prototype was formulated in the finite element software Abaqus/CAE 6.14-2 [20], using 4-node bilinear axisymmetric elements type C4X4. The size of the elements is 3.3. By exploiting the axisymmetry of the whole system, only half of the device is modelled. Lead is modelled as an elastic-perfectly plastic material, and S450 steel is assumed for shaft, tube and cap. Hard contact is introduced at the interface between shaft and tube and between shaft and cap, while hard contact in normal direction, and frictional behavior in shear direction is assumed at the interfaces between lead and shaft or tube, respectively. Dynamic implicit analyses were performed on the numerical model by imposing a cyclic displacement history to the shaft.

The numerical model correctly predicts the yield strength of the device in extension ($N_y > 0$), but underestimates the yield strength in compression, as it is unable to capture the asymmetric behavior of the specimen caused by the trailing void (Fig. 6). However, if the average yield strength on the positive and the negative branches of the loop is considered, the gap between the calculated and the experimental value is less than 15%, and the error on the energy dissipated per cycle is less than 1%. Since the experimental loop of the specimen is affected by manufacturing issues, like e.g. voids caused by entrapped air during filling with molten lead, the numerical model is deemed to provide a reliable prediction of the LED behavior for design purposes.

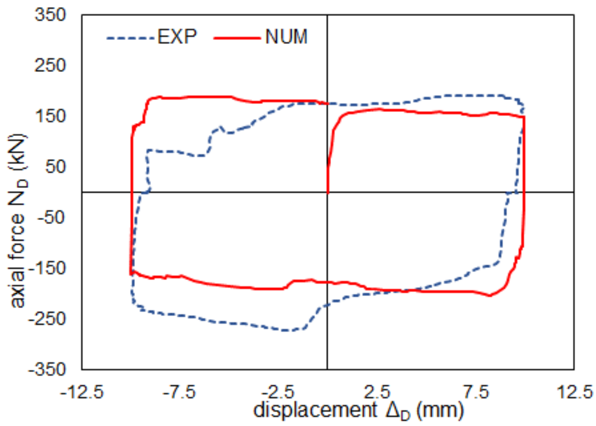

Fig. 7 – Comparison between calculated (NUM) and experimental (EXP) hysteresis loops of the LED

4.2 Parametric study

A parametric study was performed in order to investigate the influence of the design parameters of the LED on its mechanical properties. Four parameters were accounted for in the study: the diameter of the shaft, the length of the shaft in sliding contact with the lead, the diameter of the bulge, and the diameter of the tube. The ranges of variation are listed in Table 1. Force – displacement loops were calculated by using the numerical parameters presented in the previous subsection and used to derive the basic response of the LED.

Table 1 – Design parameters of LED investigated in the study

Parameter	**symbol**	**Unit**	**values**
shaft diameter	D_s	Mm	32 – 34 – 36
shaft length	L_s	Mm	43 – 63 – 83
bulge diameter	D_{bulge}	Mm	32 to 48, in 2 mm steps
tube diameter	D_t	Mm	50 – 55 – 60 mm

4.3 Results

Fig. 8(a) illustrates how the shaft diameter and the bulge diameter affect the yield strength, for fixed tube diameter and shaft length. The governing parameter is the annular area of the bulge A_{bulge}, $= \pi (D_{bulge}^2 - D_s^2)/4$, i.e. the projected face area of the bulge over which direct stress is applied to the shaft, which primarily depends on the bulge diameter, while the shaft diameter has a minor effect. As the diameter of the bulge approaches the diameter of the shaft, the contribution to the axial force due to the extrusion of lead becomes smaller, and for $D_{bulge} = D_s$ the axial force tends to a minimum value which corresponds to the friction force produced by sliding of lead on the lateral surface of the shaft.

Fig. 8(b) shows the effect of the tube diameter and of the shaft length for fixed shaft diameter. The diameter of the tube has little influence when the bulge is small, but its effect becomes important, inducing a steep increase in axial force, when the diameter of the bulge is large, as the area of the annular orifice through which the compressed lead is extruded becomes smaller. On the contrary, the effect of the shaft length is shown to be relatively small (on the order of 25-30 kN for a 20 mm change in length) and independent of the bulge diameter. Increasing the shaft length entails indeed a proportional increase in the

the area of the lateral surface of the shaft in sliding contact with the working material and consequently of the friction force developed by lead.

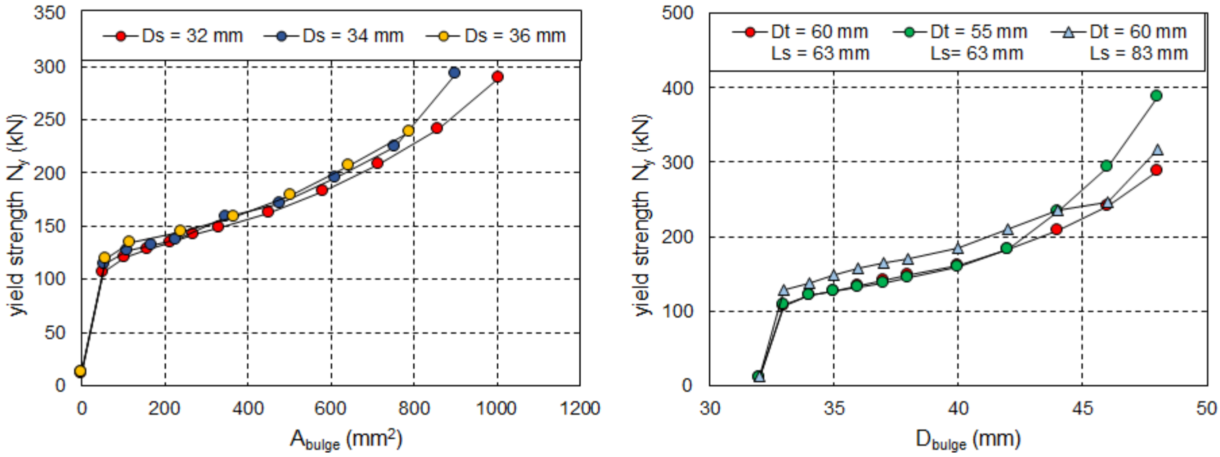

(a) (b)

Fig. 8 – Influence of design parameters on LED yield strength N_y: (a) influence of shaft diameter D_s and annular area of the bulge A_{bulge} for assigned tube diameter D_t = 60 mm and shaft length L_s = 63 mm; (b) influence of tube diameter D_t and shaft length L_s for assigned shaft diameter D_s = 32 mm

5. LED with Adaptive Behavior

A novel Adaptive Lead Extrusion Damper (ALED) has been developed within the study. The ALED is designed to provide two distinct strength levels depending on the shaft displacement, with the aim of modifying the response of the structure in which it is provided according to the magnitude of the deformations induced by the ground motion. Tests performed on a pilot prototype demonstrate the ability of the ALED to provide a substantial change in the resisting force when a threshold deflection is exceeded, adapting its strength and damping characteristics to the accommodated displacement. By referring to the loops shown in Fig. 9, the device indeed exhibits a “two-steps” rigid plastic response, characterized by a “level-1” strength of 80 kN for small displacements (Δ_D < 5 mm), followed by a “level-2” strength of 150 kN for 5 < Δ_D < 10 mm.

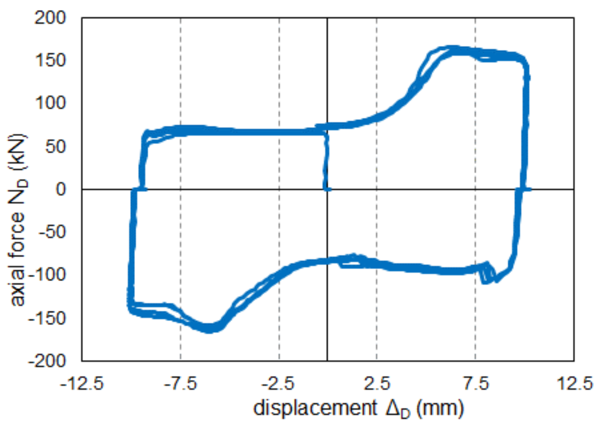

Fig. 9 – Hysteresis loop of the ALED

6. Conclusions

The Lead Extrusion Damper (LED) has been experimentally and numerically investigated in the study. The device provides a resistive force by plastically extruding lead through an orifice created by an annular restriction between a tube and a bulged shaft.

A prototype of the LED was manufactured to perform the experimental investigation. The device features a compact design, with smaller dimensions than hysteretic devices with equivalent performance. Cyclic tests according to EN 15129 were performed to obtain the basic characteristics for different displacement amplitudes. The damper exhibits a consistent rigid-plastic behavior without significant strength degradation. In spite of some minor trailing voids which can be managed by design in an improved version of the device, the hysteresis loops have an essentially rectangular shape with an equivalent damping ratio of 0.55, close to the maximum theoretical value of 0.63. The damper was able to sustain multiple sequences of motion at the basic design earthquake displacement, demonstrating maintenance-free operation even in presence of repeated ground shakes.

A 3D finite element model of the LED was formulated and used, in a parametric study, to investigate the effect of the design parameters on the mechanical response of the device. It is shown that the main parameter governing the response of the LED is the annular area of the bulge A_{bulge}, that represents the projected face area of the bulge over which direct stress is applied to the shaft. The results of the parametric analyses can be used to draw design charts to assist the manufacturers for the preliminary design of the system.

Eventually, a novel Adaptive Lead Extrusion Damper (ALED) was assessed in pilot tests. The preliminary results demonstrate the ability of the ALED to provide a “two-steps” rigid-plastic loop, with a substantial increase in the resisting force when a certain displacement is exceeded. The ALED can be used in structures to modify their response depending on the magnitude of the ground motion.

7. References

[1] Muto K (1969): Earthquake resistant design of 36-storied Kasumigaseki Building. *4th World Conference on Earthquake Engineering*, Santiago, Chile.

[2] Kelly JM, Skinner RI, Heine AJ (1972): Mechanisms of energy absorption in special devices for use in earthquake resistant structures. *Bulletin of the New Zealand National Society for Earthquake Engineering*, **5**(3), 53-68.

[3] Skinner RI, Kelly JM, Heine AJ (1974): Hysteretic dampers for earthquake-resistant structures. *Earthquake Engineering and Structural Dynamics*, **3**(3), 287-296.

[4] Christopolous C, Filiatrault A (2006): *Principles of passive supplemental damping and seismic isolation*. IUSS Press, Pavia.

[5] Robinson WH, Greenbank LR (1975): Properties of an extrusion energy absorber. *Bulletin of the New Zealand National Society for Earthquake Engineering*, **8**(3), 187-191.

[6] Rodgers GW, Chase JG, Mander JB, Leach NC, Denmead CS (2007): Experimental development, tradeoff analysis and design implementation of high force-to-volume damping technology. *Bulletin of the New Zealand National Society for Earthquake Engineering*, **40**(2), 35-48.

[7] Rodgers GW (2009): Next generation structural technologies: implementing high force-to-volume energy absorbers *Ph.D. Thesis*, University of Canterbury, Christchurch, New Zealand.

[8] Rodgers GW, Chase JG (2013): Testing of Lead Extrusion Damping devices undergoing representative earthquake velocities. *2013 NZSEE Conference*, Wellington, New Zealand.

[9] Soydan C, Yüksel E, İrtem E (2017): Determination of the characteristics of a new prestressed Lead Extrusion Damper. *16th World Conference on Earthquake Engineering*, Santiago, Chile.

[10] Soydan C, Yüksel E, İrtem E (2018): Retrofitting of pinned beam–column connections in RC precast frames using lead extrusion dampers. *Bulletin of Earthquake Engineering*, 16, 1273.

[11] Latham DA, Reay AM, Pampanin S (2013): Kilmore Street Medical Centre: Application of an Advanced Flag-Shape Steel Rocking System. *2013 NZSEE Conference*, Wellington, New Zealand.

[12] Cousins WJ, Porritt TE (1993): Improvements to lead-extrusion damper technology. *Bulletin of the New Zealand National Society for Earthquake Engineering*, **26**(3), 342-348.

[13] CEN 15129 (2009): *Antiseismic Devices*. European Centre for Normalization.

[14] Robinson WH, Greenbank LR (1976): Extrusion energy absorber suitable for the protection of structures during an earthquake. *Earthquake Engineering & Structural Dynamics*, **4**(3), 251-259.

[15] Robinson WH, Cousins WJ (1987): Recent developments in lead dampers for base isolation. *Proceedings of the Pacific Conference On Earthquake Engineering*, 2, 279-283.

[16] Sadek F, Mohraz B, Taylor AW, Chung RM (1996): Passive energy dissipating devices for sesismic applications. *Report NISTIR 5923*, Building and Fire Research Laboratory, National Institute of Standards and Technology, Gaithersburg, Maryland, USA.

[17] Wulf J, Taylor JF, Shaler AJ (1956): *Metallurgy for Engineers*. John Wiley and Sons, New York.

[18] Birchenall CE (1959): *Physical Metallurgy*. McGraw-Hill, London.

[19] Dassault Systèmes Simulia (2014): *ABAQUS/Analysis User's Guide, Version 6.14*. Providence.

